P H Y S I C A L   R E V I E W   L E T T E R S

Polariton Condensation with Localized Excitons and Propagating Photons

Jonathan Keeling, P. R. Eastham, M. H. Szymanska, and P. B. Littlewood

Cavendish Laboratory, Madingley Road, Cambridge CB3 OHE, United Kingdom

We estimate the condensation temperature for microcavity polaritons, allowing for their internal structure. We consider polaritons formed from localized excitons in a planar microcavity, using a generalized Dicke model. At low densities, we find a condensation temperature $T_c \propto \rho$, as expected for a gas of structureless polaritons. However, as T_c becomes of the order of the Rabi splitting, the structure of the polaritons becomes relevant, and the condensation temperature is that of a BCS-like mean-field theory. We also calculate the excitation spectrum, which is related to observable quantities such as the luminescence and absorption spectra.

Bose condensation of polaritons in two-dimensional semiconductor microcavities has been the object of continuing experiments. Recent progress includes observations of a nonlinear increase in the occupation of the ground state [1,2], subthermal second order coherence [2], changes to the momentum distribution of polaritons [3], and stimulated processes in resonantly pumped cavities [4]. However, unambiguous evidence for the existence of a polariton condensate is still lacking. Theoretical predictions of the conditions required for condensation, and of signatures of condensation, are therefore of great interest. We find that the momentum distribution of radiation from the cavity shows a dramatic change when condensed , which, together with the gap in the luminescence, could provide such signatures.

Because of the small polariton mass, a weakly interacting Bose gas of polaritons predicts extremely high transition temperatures, which provides the motivation for studying polariton condensation; see [5] and references therein. At such high temperatures, when T_c is of the order of the Rabi splitting, the internal structure of the polariton becomes relevant, and treating polaritons as structureless bosons fails. This can occur at density scales much less than the exciton saturation (Mott) density; while current experiments [3] are well below the Mott density, they are at densities where the internal structure is relevant.

In this Letter, we study polariton condensation in thermal equilibrium, including polariton internal structure. Although current experiments may not have reached equilibrium, this remains their aim; further the signatures of equilibrium condensation are instructive when considering the nonequilibrium case. We consider a model of localized excitons in a two-dimensional microcavity, building on previous studies of zero-dimensional microcavities [6]. This is motivated by experimental systems such as organic semiconductors [7], quantum dots [8], and disordered quantum wells [9]. Moreover, it has been argued [10] that exciton localization might aid condensation; inhomogeneous broadening due to localization suppresses condensation less than the homogeneous de-

phasing for propagating excitons. Finally, since the exciton mass is much larger than the photon mass, we expect much of the physics of condensation in the localized exciton model to carry over to systems with propagating excitons, for densities much less than the Mott density.

For simplicity, we model the localized excitons as isolated two-level systems, with the two states corresponding to the presence or absence of an exciton on a particular site. A two-level system will be represented as a fermion occupying one of two levels, further constrained so that the total occupation of a site is one. This constraint describes a hard-core repulsion between excitons on a single site; we neglect Coulomb interactions between different sites as being small compared to the photon mediated interaction. In a two-dimensional microcavity, the photon dispersion relation for low k is $\hbar\omega_k = \hbar\omega_0 + \hbar^2 k^2/2m$, where $m = (\hbar/c)(2\pi/w)$ for a cavity width w. Each mode couples to all excitons, with different phases. Describing the coupling in the electric dipole gauge, the coupling strength is $g = d_{ab}\sqrt{2\pi\hbar\omega_k}$, in which we approximate $\omega_k \approx \omega_0$, and d_{ab} is the dipole moment. These considerations lead to the generalized Dicke Hamiltonian[11]

$$H = \sum_{j=1}^{j=nA} \epsilon_j (b_j^\dagger b_j - a_j^\dagger a_j) + \sum_{k=2\pi l/\sqrt{A}} \hbar\omega_k \psi_k^\dagger \psi_k$$
$$+ \frac{g}{\sqrt{A}} \sum_{j,k} (e^{2\pi i \mathbf{k}\cdot\mathbf{r}_j} \psi_k a_j^\dagger b_j + e^{-2\pi i \mathbf{k}\cdot\mathbf{r}_j} \psi_k^\dagger b_j^\dagger a_j). \quad (1)$$

Here $A \to \infty$ is the quantization area and n the areal density of two-level systems, i.e., sites where an exciton may exist. Without inhomogeneous broadening, the energy of a bound exciton is $2\epsilon = \Delta + \omega_0$, defining the detuning Δ between the exciton and the photon. The grand canonical ensemble, $\tilde{H} = H - \mu N$, allows the calculation of equilibrium for a fixed total number of excitations (excitons and photons);

$$N = \sum_{j=1}^{j=nA} \frac{1}{2}(b_j^\dagger b_j - a_j^\dagger a_j + 1) + \sum_{k=2\pi l/\sqrt{A}} \psi_k^\dagger \psi_k. \quad (2)$$

We therefore define $\tilde{\omega}_k = \omega_k - \mu$ and $\tilde{\epsilon} = \epsilon - \mu/2$. If $\mu = 0$, this Hamiltonian is an extension of that studied by Hepp and Lieb [12], as discussed further in [6].

Using the characteristic density, n, and energy scale $g\sqrt{n}$ (the Rabi splitting), the system is controlled by two dimensionless parameters: detuning, $\Delta^* = \Delta/g\sqrt{n}$, and photon mass, $m^* = mg/\hbar^2\sqrt{n}$. For the system in Ref. [2], $g\sqrt{n} \approx 20$ meV, $\hbar\omega_0 \approx 1.6$ eV, and $m \approx 10^{-5}m_e$. For delocalized but interacting excitons, assuming that the exciton-exciton interaction is a hard-core repulsion on the scale of the Bohr radius gives an upper bound on the density of available exciton sites as $n \approx 10^{11}n_{QW}$ cm^{-2}, where n_{QW} is the number of quantum wells in the cavity. These values lead to dimensionless parameters $m^* \approx 10^{-3}$, and by design $\Delta^* = 0$. The quoted exciton densities in Ref. [3] are $\approx 10^9$ cm^{-2} per well, leading us to estimate the fraction of occupied exciton sites to be less than 10^{-2}. Using these values, our work suggests (see Fig. 4) that current experiments [3] are in the interaction dominated mean-field regime.

Using the standard functional path integral techniques for the partition function as in [6] and integrating over the fermion fields yields an effective action for photons:

$$S[\psi] = \int_0^\beta d\tau \sum_k \psi_k^\dagger (\partial_\tau + \hbar\tilde{\omega}_k)\psi_k - N\mathrm{Tr}\ln(\mathcal{M}) \quad (3)$$

$$\mathcal{M}^{-1} = \begin{pmatrix} \partial_\tau + \tilde{\epsilon} & \frac{g}{\sqrt{A}}\sum_k e^{2\pi i \mathbf{k}\cdot\mathbf{r}_j}\psi_k \\ \frac{g}{\sqrt{A}}\sum_k e^{-2\pi i \mathbf{k}\cdot\mathbf{r}_j}\bar{\psi}_k & \partial_\tau - \tilde{\epsilon} \end{pmatrix}.$$

We then proceed by minimizing $S[\psi]$ with a static uniform ψ and expanding around this minimum. The minimum, ψ_0, satisfies the equation:

$$\tilde{\omega}_0\psi_0 = g^2 n \frac{\tanh(\beta E)}{2E}\psi_0, \qquad E = \sqrt{\tilde{\epsilon}^2 + g^2 n|\psi_0|^2}, \quad (4)$$

which describes the mean-field condensate of coupled coherent photons and exciton polarization studied in [6].

To consider the influence of incoherent fluctuations, we expand the logarithm in Eq. (3) for fluctuations $\psi = \psi_0 + \delta\psi$ and obtain a contribution to the action: $\frac{1}{2}\mathrm{Tr}(\mathcal{M}\delta\mathcal{M}^{-1}\mathcal{M}\delta\mathcal{M}^{-1})$. This, with the bare photon action, yields the inverse Greens function for photon fluctuations $\mathcal{G}^{-1}(\omega, k)$. The resultant expression has terms proportional to δ_ω. These arise from second order poles in the Matsubara summation; such terms vanish on analytic continuation, and so do not affect the retarded Greens function.

The Greens function has poles, representing the energy of excitations with respect to the chemical potential. In the normal state there are two poles which describe the upper and lower polariton dispersion

$$E_\pm = \frac{1}{2}\left[(\tilde{\omega}_k + 2\tilde{\epsilon}) \pm \sqrt{(\tilde{\omega}_k - 2\tilde{\epsilon})^2 + 4g^2 n \tanh(\beta\tilde{\epsilon})}\right] \quad (5)$$

and are presented in Fig. 1. The polariton dispersion (5) from localized excitons has the same structure as from propagating excitons, since the photon dispersion dominates. In the condensed state, the excitation spectrum changes dramatically (see Fig. 1). There are four poles, reflecting the symmetry of adding or subtracting a particle in the presence of the condensate:

$$\xi_{1,2}^2 = \frac{1}{2}\left[A(k) \pm \sqrt{A(k)^2 - 16\frac{k^2}{2m}\left(\frac{E^2 k^2}{2m} + B\right)}\right]$$

$$A(k) = 4E^2 + \tilde{\omega}_k^2 + 4\tilde{\epsilon}\tilde{\omega}_0, \qquad B = g^2 n \frac{|\psi|^2}{N}\tilde{\omega}_0. \quad (6)$$

At low k, the inner lines correspond to changing the phase of the condensate. At higher k, unlike in BCS superconductivity, amplitude and phase modes get mixed.

For small momenta, the phase mode is linear, $\xi_1 = \pm ck + O(k^2)$. The phase velocity has the form

$$c = \sqrt{\frac{1}{2m}\left(\frac{4\tilde{\omega}_0 g^2 n}{\xi_2(0)^2}\right)\left(\frac{|\psi_0|^2}{N}\right)} \approx \sqrt{\frac{\lambda}{2m}\frac{\rho_0}{n}} \quad (7)$$

where the second expression is for comparison the form for a dilute Bose gas with contact interaction λ. The phase velocity increases for small ψ_0 then decreases as saturation of the excitons reduces the effective exciton-photon interaction strength.

The difference in the structure of the excitation spectra between condensed and uncondensed states may be seen in the luminescence spectra and in the angle-resolved luminescence $N(k)$. Although four poles exist, they may have very different spectral weights, and would therefore show up differently in optical measurement. This can be understood more clearly after introducing inhomogeneous broadening of the exciton energies, which broadens the poles. In this case, one may plot the spectral weight of the photon greens function, $2\Im[\mathcal{G}(i\omega = z + i\eta)]$ as $\eta \to 0$, which corresponds experimentally to the absorption
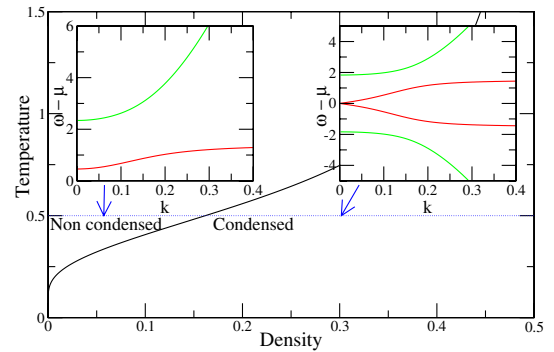

FIG. 1 (color online). Condensed and uncondensed spectra, superimposed on the mean-field phase diagram to show choice of mean-field density and temperature. (Parameters $\Delta^* = 0$, $m^* = 0.01$. $\mu/g\sqrt{n} = -1.4$ below transition; $\mu/g\sqrt{n} = -0.6$ above. Energies and densities plotted in units of $g\sqrt{n}$ and n.)

coefficient. Figure 2 shows this for the same parameters as Fig. 1.

In the condensed case, there are three bright lines above the chemical potential: the Goldstone mode (which is not broadened as it lies inside the gap for single particle excitations), the edge of the gap, and the broadened upper polariton mode. If the inhomogeneous broadening is large, the gap edge peak and upper polariton will be broadened. This will result in a band of incoherent luminescence separated from the coherent emission at the chemical potential by the gap. If the broadening is small with respect to the gap, then very little structure will be seen. Such structure can, however, still be seen at low densities.

The momentum distribution of photons may also be found from the photon Greens function. This is characteristic of the angular distribution of radiation; if reflectivity of the mirrors were independent of angle, and approximating $\omega_k \approx \omega_0$, then $\sin(\theta) = ck/\omega_0$. The momentum distribution is given by:

$$N(k) = \lim_{\eta \to 0} \langle \psi_k^\dagger(\tau + \eta)\psi_k(\tau) \rangle. \qquad (8)$$

Although the system is two-dimensional, a condensed momentum distribution can be calculated at low temperatures by considering only phase fluctuations [13]. Figure 3 shows this for both condensed and uncondensed states. The linear phase mode leads to a power law divergence at low momenta, becoming sharper as the temperature decreases.

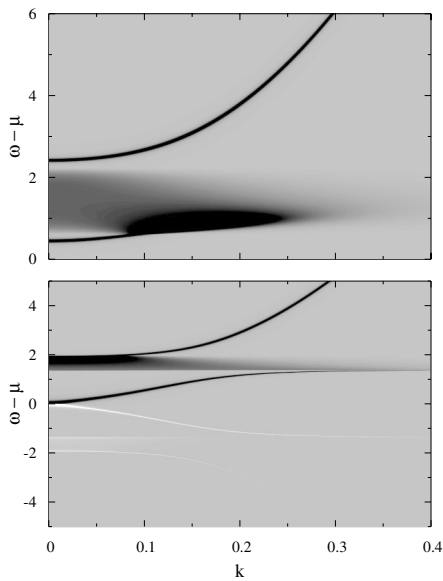We now estimate the phase boundary, including the effects of fluctuations. We calculate the free energy from the action in Eq. (3), evaluated to Gaussian order. Taking the total derivative of free energy with respect to chemical potential gives the total density, and evaluating this at the critical chemical potential gives an estimate of the phase boundary. This follows the method of [14], but is complicated by the effects of a dynamic boson field and by two-dimensionality.

The total density is

$$\rho = \frac{n}{2}\left[1 - \frac{\tilde{\epsilon}}{E}\tanh(\beta E) \right] + \frac{|\psi_0|^2}{A}$$
$$+ \int_0^K (dk)^2[f(\xi_1) + f(\xi_2) - f(2E) + g(k)] \qquad (9)$$

when condensed, with $f(x) = -[n_B(x) + 1/2]dx/d\mu$, and $g(k)$ due to δ_ω; and

$$\rho = \frac{n}{1 + e^{2\beta\tilde{\epsilon}}} + \int_0^K (dk)^2[f(E_+) + f(E_-) - f(2\tilde{\epsilon})], \quad (10)$$

with $f(x) = -n_B(x)dx/d\mu$, when uncondensed.

Considering the terms in Eq. (9), these can be identified as exciton density and coherent photon density on the first line. Under the integral are the occupation of upper and lower polaritons, and subtraction of exciton density, required as excitons would otherwise be counted twice. The cutoff K regularizes the ultraviolet divergence. The theory is not renormalizable, due to the constant coupling between high energy photon modes and the excitons; but for low energy properties, changing the cutoff introduces only small corrections.

However, as well as changing density, fluctuations change the critical chemical potential by depleting the condensate [15]. Therefore, it is necessary to make a separate estimate of the condensate density including fluctuations. For a two-dimensional system, this can be achieved by calculating the superfluid response, which requires comparing the transverse (normal) response, and the total density:

FIG. 2. Absorption coefficient vs momentum (x axis) and energy (y axis) calculated above (top) and below (bottom) phase transition. Negative values indicate gain. (Parameters as for Fig. 1, inhomogeneous broadening width $0.3g\sqrt{n}$.) The color scale covers the range $-\infty$ to ∞.
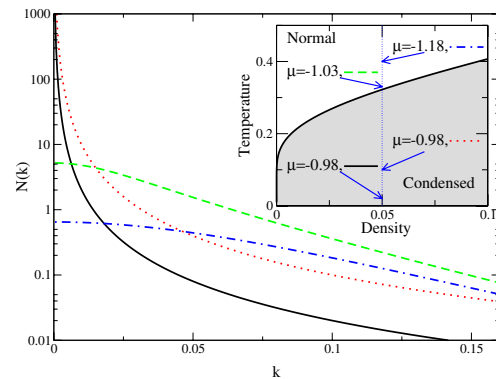

FIG. 3 (color online). Momentum distribution of photons, from which follows the angular distribution. Two uncondensed and two condensed distributions are shown for mean-field densities as shown in the inset. (Parameters $\Delta^* = 0$, $m^* = 0.01$.)
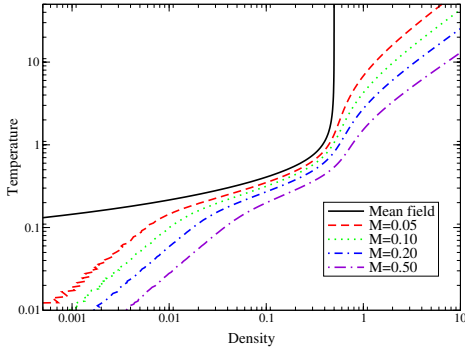
FIG. 4 (color online). Phase boundaries calculated from mean-field theory, and including fluctuation corrections for four different values of photon mass. Temperature and density plotted in units of $g\sqrt{n}$ and n.

$$\rho_s = \rho_p - \rho_n, \qquad \rho_n = \frac{1}{m\beta A}\lim_{q\to 0}\left[\left(\delta_{ij} - \frac{q_i q_j}{q^2}\right)\chi_{ij}(q)\right]$$

$$\chi_{ij}(q) = \mathrm{Tr}\left[\frac{k_i k_j}{2}\mathcal{G}\left(\omega, k - \frac{q}{2}\right)\sigma_3\mathcal{G}\left(\omega, k + \frac{q}{2}\right)\sigma_3\right], \quad (11)$$

where $\mathcal{G}$ is the photon greens function and ρ_p is the total photon density. The transverse response may be safely calculated without vertex corrections, as these affect only the longitudinal response. Combining the results of Eqs. (9) and (11), the phase transition including fluctuations occurs when $\rho_s = 0$. As the system is two-dimensional, one ought to consider a Kosterlitz-Thouless transition, at finite ρ_s, but this introduces only small corrections. The phase boundaries for four different photon masses are shown in Fig. 4.

At low densities, the phase transition occurs as the condensate is depleted by occupation of the phase mode. Therefore, the phase boundary has the form $T_c \propto \rho/m_{\mathrm{pol}}$ where m_{pol} is the polariton mass, which, at resonance, is just $2m$. This compares to the mean-field boundary, which at resonance is

$$T_c = g\sqrt{n}\frac{\sqrt{1 - 2\rho}}{2\tanh^{-1}(1 - 2\rho)} \approx \frac{g\sqrt{n}}{-\ln\rho}, \qquad (12)$$

the second equality being valid for small densities. This temperature is effectively constant on the scale of the BEC phase boundary.

As the density increases, the phase boundary including fluctuations will approach the mean-field boundary. Because of the slow dependence of the mean-field boundary on density, this will occur at $T \approx g\sqrt{n}$, unless mass is very large. The exact temperature where this occurs depends on the mass. For a small mass, the fluctuation boundary follows the mean-field boundary over a wider range of densities. The rescaled photon mass, m^*, provides a small parameter near $T \approx g\sqrt{n}$, $\rho \approx n$. Physically, at a temperature scale of $g\sqrt{n}$, the fluctuation modes are occupied to the top of the lower polariton branch, and occupation of the upper branch becomes relevant.

At yet higher densities, the fluctuation result again differs from the mean field. For $\rho > n$, the mean-field theory will always predict a condensate. However, at high densities, the system is dominated by incoherent photons not described in the mean-field theory. In this limit, the phase boundary is that for BEC of (massive) photons.

To conclude, we have calculated the spectrum of fluctuations for a model of localized excitons interacting with propagating photons. In the condensed state, the fluctuations about mean field include the Goldstone mode, and the linear dispersion causes a characteristic change to the momentum distribution of photons. Both the narrowing of the $N(k)$ distribution and the gap between coherent and incoherent luminescence would provide evidence for polariton condensation. Fluctuations alter the form of the phase transition. At low densities, the transition has the $T_c \propto \rho$ form expected for Bose condensation of preformed bosons. As the density increases for small masses, the mean-field interaction driven limit is recovered for densities $\rho \approx n$. However, for yet higher densities, the boundary changes again to Bose condensation of weakly interacting photons.

[1] L. S. Dang, D. Heger, R. André, F. Bœuf, and R. Romestain, Phys. Rev. Lett. **81**, 3920 (1998).
[2] H. Deng, G. Weihs, C. Santori, J. Bloch, and Y. Yamamoto, Science **298**, 199 (2002).
[3] H. Deng, G. Weihs, D. Snoke, J. Bloch, and Y. Yamamoto, Proc. Natl. Acad. Sci. U.S.A. **100**, 15318 (2003).
[4] P. G. Savvidis, J. J. Baumberg, R. M. Stevenson, M. S. Skolnick, D. M. Whittaker, and J. S. Roberts, Phys. Rev. Lett. **84**, 1547 (2000).
[5] A. Kavokin, G. Malpuech, and F. P. Laussy, Phys. Lett. A **306**, 187 (2003).
[6] P. R. Eastham and P. B. Littlewood, Phys. Rev. B **64**, 235101 (2001).
[7] D. G. Lidzey et al., Phys. Rev. Lett. **82**, 3316 (1999).
[8] U. Woggon et al., Appl. Phys. B **77**, 469 (2003).
[9] H. F. Hess, E. Betzig, T. D. Harris, L. N. Pfeiffer, and K. W. West, Science **264**, 1740 (1994).
[10] M. H. Szymanska, P. B. Littlewood, and B. D. Simons, Phys. Rev. A **68**, 013818 (2003).
[11] R. H. Dicke, Phys. Rev. **93**, 99 (1954).
[12] K. Hepp and E. Lieb, Phys. Rev. A **8**, 2517 (1973).
[13] J. Keeling, L. S. Levitov, and P. B. Littlewood, Phys. Rev. Lett. **92**, 176402 (2004).
[14] P. Nozières and S. Schmitt-Rink, J. Low Temp. Phys. **59**, 195 (1985).
[15] V. N. Popov, *Functional Integrals in Quantum Field Theory and Statistical Physics* (Reidel, Dordrecht, 1983), Chap. 6.